



Sodium ionic conductivity and stability of amorphous $\text{Na}_2\text{O} \cdot 2\text{SiO}_2$ added with M_xO_y ($\text{M} = \text{Zr}, \text{Y}$, and Sm)

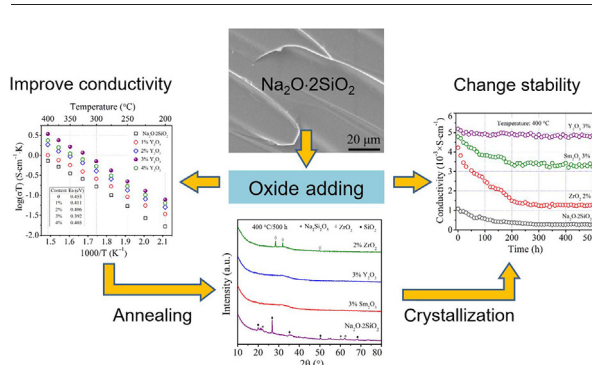
Shan-Lin Zhang, Xiao-Na Wang, Cheng-Xin Li *, Chang-Jiu Li

State Key laboratory for Mechanical Behavior of Materials, School of Materials Science and Engineering, Xi'an Jiaotong University, Xi'an, Shaanxi 710049, China

HIGHLIGHTS

- Oxides adding can change the network structure and physical properties of $\text{A-Na}_2\text{O} \cdot 2\text{SiO}_2$ significantly.
- The ionic conductivity of $\text{A-Na}_2\text{O} \cdot 2\text{SiO}_2$ increased ~5 times by adding 3 mol% Y_2O_3 .
- The conductivity of 3 mol% Y_2O_3 -added $\text{A-Na}_2\text{O} \cdot 2\text{SiO}_2$ at 400 °C almost not changed after 500 h annealing
- Conductivity degradation of $\text{A-Na}_2\text{O} \cdot 2\text{SiO}_2$ can be attributed to the crystallization.

GRAPHICAL ABSTRACT



ARTICLE INFO

Article history:

Received 11 October 2017

Received in revised form 19 January 2018

Accepted 21 January 2018

Available online 31 January 2018

Keywords:

Ionic conductor

Amorphous $\text{Na}_2\text{O} \cdot 2\text{SiO}_2$

Oxide adding

Conductivity

Thermal stability

ABSTRACT

Amorphous $\text{Na}_2\text{O} \cdot 2\text{SiO}_2$ ($\text{A-Na}_2\text{O} \cdot 2\text{SiO}_2$) is one of the promising sodium ionic conductors for solid-state sodium-ion battery electrolytes owing to its easy preparation and low production cost. However, $\text{Na}_2\text{O} \cdot 2\text{SiO}_2$ glass suffers from relatively low conductivity and poor thermal stability as a result of crystallization and other defects. Herein, we improved the ionic conductivity and thermal stability of $\text{A-Na}_2\text{O} \cdot 2\text{SiO}_2$ by adding this material with metal oxides (M_xO_y , $\text{M} = \text{Y}$, Sm , and Zr) at varying loadings. The physical properties and stability of the $\text{A-Na}_2\text{O} \cdot 2\text{SiO}_2$ added with different oxides were systematically investigated. The results indicated that oxide adding on $\text{A-Na}_2\text{O} \cdot 2\text{SiO}_2$ resulted in larger density values that increased with the adding content. Additionally, oxide adding changed the strength of the Si—O bond in $\text{A-Na}_2\text{O} \cdot 2\text{SiO}_2$, thereby affecting the overall network structure and uniformity. Among the different oxides prepared, added with 3 mol% Sm_2O_3 , 3 mol% Y_2O_3 , and 2 mol% ZrO_2 showed maximum hardness and elasticity modulus values. Additionally, oxide adding on $\text{A-Na}_2\text{O} \cdot 2\text{SiO}_2$ resulted in significantly improved ionic conductivity values. 3 mol% Y_2O_3 -added $\text{A-Na}_2\text{O} \cdot 2\text{SiO}_2$ material showed the highest ionic conductivity value ($5.2 \times 10^{-3} \text{ S cm}^{-1}$) and optimum thermal stability, indicating that Y_2O_3 -added $\text{Na}_2\text{O} \cdot 2\text{SiO}_2$ has high potential to be high-performance and stable sodium ionic conductors.

© 2018 Elsevier Ltd. All rights reserved.

1. Introduction

Solid-state fast-ion conductors are important functional electrolyte materials for high-power, high-capacity, and efficient solid electrochemical cells (e.g., fuel cells [1] and batteries [2]) used in a variety of

energy applications. The high ionic conductivity of these materials, comparable to those of liquid electrolytes [3], originates from a specific structure that enables easy diffusion of conducting ions. New fast-ion conducting electrolytes with superior conductivity values have been discovered after several decades of research. In recent years, Singh and Goodenough et al. reported on a Na-doped SrSiO_3 material combining high ionic conductivity and good stability at high temperatures [4–6], although the conducting mechanism remained unclear. According to

* Corresponding author.

E-mail address: licx@mail.xjtu.edu.cn (C.-X. Li).

the subsequent studies reported by Bayliss [7,8], Evans [9], Tealdi [10], and Huang [11,12] et al., Na-doped SrSiO_3 form two phases (i.e., Na-doped SrSiO_3 in minor amounts and amorphous $\text{Na}_2\text{O} \cdot 2\text{SiO}_2$ ($\text{A-Na}_2\text{O} \cdot 2\text{SiO}_2$)) during the sintering or reaction processes. These authors revealed $\text{A-Na}_2\text{O} \cdot 2\text{SiO}_2$ to be the main conductive phase in the composite material, which was confirmed to be a Na^+ (instead of O^{2-}) conductor. Owing to its high Na^+ conductivities (over 0.02 S cm^{-1} at 500°C) [13], $\text{A-Na}_2\text{O} \cdot 2\text{SiO}_2$ is a highly promising material for Na—S cell [14] and carbon dioxide sensor applications.

Compared with other Na^+ ionic conducting ceramics such as $\beta''\text{-Al}_2\text{O}_3$ [15] and $\text{Na}_3\text{Zr}_2\text{Si}_2\text{PO}_{12}$ widely used as solid-state electrolytes for Na—S cells and carbon dioxide sensors [16–18], $\text{A-Na}_2\text{O} \cdot 2\text{SiO}_2$ has numerous advantages (e.g., lower material costs and lower sintering temperatures). However, $\text{A-Na}_2\text{O} \cdot 2\text{SiO}_2$ shows relatively lower conductivities as compared to $\beta''\text{-Al}_2\text{O}_3$ and $\text{Na}_3\text{Zr}_2\text{Si}_2\text{PO}_{12}$ (4.2×10^{-2} and $6.7 \times 10^{-2} \text{ S cm}^{-1}$ at 200°C , respectively). Additionally, according to Jee et al. [13], crystallization of $\text{A-Na}_2\text{O} \cdot 2\text{SiO}_2$ at high temperatures has a significant detrimental effect on conductivity. Thus, at 500°C , $\text{A-Na}_2\text{O} \cdot 2\text{SiO}_2$ showed a sharp decrease in conductivity within the first 24 h and gradually decreased thereafter to less than 10% of the initial conductivity [13]. Therefore, two critical challenges, achieving higher conductivities and improving the long-term stability, are required for high-performance Na^+ conducting electrolytes before being applied commercially.

Oxide adding is a proper method to improve the properties and stability of amorphous glass by altering its network structure [19–22]. As reported by K. Thieme and Rüssel [23], CeO_2 or Y_2O_3 can be used as nucleation inhibitors for lithium disilicate glasses (i.e., $\text{A-Li}_2\text{O} \cdot 2\text{SiO}_2$). These authors also reported that Nb_2O_5 or Ta_2O_5 adding can also change the crystallization behavior of $\text{Li}_2\text{O} \cdot 2\text{SiO}_2$ glass [24]. Moreover, Kiyono et al. [19] performed Y_2O_3 adding on sodium ion conducting silicate glass to improve its water corrosion resistance. Therefore, oxide adding can greatly improve the conductivity and stability of $\text{A-Na}_2\text{O} \cdot 2\text{SiO}_2$.

In the present study, we selected three different oxides (i.e., ZrO_2 , Y_2O_3 , and Sm_2O_3) as adding materials for $\text{A-Na}_2\text{O} \cdot 2\text{SiO}_2$. With the aim to ensure that the samples remained in the amorphous-forming region during the synthesis process, these oxides were added at limited amounts of 1–4 mol%. First, the effect of oxide adding on the physical and mechanical properties (i.e., density, hardness, and elastic modulus) of the oxides-added $\text{A-Na}_2\text{O} \cdot 2\text{SiO}_2$ materials were investigated. Fourier transform infrared spectroscopy (FT-IR) was subsequently used to analyze the changes in the glass network structure induced by oxide adding. Finally, the conductivity and long-term stability of the oxides-added $\text{Na}_2\text{O} \cdot 2\text{SiO}_2$ samples were systematically studied.

2. Experimental

2.1. Sample preparation

Commercially available 99.99% purity Na_2CO_3 , SiO_2 , Y_2O_3 , Sm_2O_3 , and ZrO_2 powders (SCRC) were used as the starting materials. Na_2CO_3 , SiO_2 , and M_xO_y ($\text{M} = \text{Zr}, \text{Y}, \text{and Sm}$) were ball-milled in ethanol for 10 h at varying compositions of $z\text{M}_x\text{O}_y$ ($100 - z$) $\text{Na}_2\text{O} \cdot 2\text{SiO}_2$ ($z = 0, 1, 2, 3, \text{ and } 4 \text{ mol}\%$). The as-prepared slurry was dried at 80°C and the obtained mixed powders were heated in air at 1350°C for 1 h in a platinum crucible. After heating, the melt was quenched on a steel plate and press formed. Finally, the as-obtained glass was incised to pellets with a size of $10 \text{ mm} \times 10 \text{ mm} \times 1 \text{ mm}$.

2.2. Characterization of the physical and mechanical properties

The density was determined by the Archimedes method in all cases. The precision of the scale used in this study was 0.001 N. The microhardness of the samples was measured with a Vickers Indenter (BUEHLER MICROMET5104, Akashi Corporation, Japan). During the test, a load of 0.98 N was used with a holding time of 15 s. The elastic modulus of

the samples was measured by the Knoop indentation method [25]. The surface of the samples was polished before testing. The load and holding time were set to 0.98 N and 15 s, respectively.

2.3. X-ray diffraction (XRD), FT-IR, and thermogravimetric/differential scanning calorimetry (TG/DSC) results

XRD analysis (Shimadzu/XRD-6000) was used to identify the phase composition of the prepared samples. Additionally, FT-IR (IRPrestige-21) analysis ($400\text{--}4000 \text{ cm}^{-1}$) was carried out to analyze the effects of oxide adding on the network structure. Before the measurements, glass bulks were ball-milled to small particles and subsequently pressed into small pellets containing KBr powders in a weight ratio of 1:200. The glass transition and crystallization temperatures (T_g and T_c , respectively) were measured by TG/DSC (NETZSCH model STA 449C). The DSC measurements were carried out with powdered samples placed on a platinum pan at a fixed temperature of 600°C with a heating rate of $10^\circ\text{C min}^{-1}$ in air. Baseline corrections were performed after the experiments.

2.4. Conductivity and long-term stability characterization

The ionic conductivities of the oxide-added $\text{A-Na}_2\text{O} \cdot 2\text{SiO}_2$ samples were measured by impedance spectroscopy (Solartron SI 1260/1287 impedance analyzer) in the frequency range of 1 Hz–1 MHz with an applied AC voltage of 25 mV. The sample size was $10 \text{ mm} \times 10 \text{ mm} \times 1 \text{ mm}$. Before testing, silver layers were attached as electrodes to both sides of the samples with silver paste. Besides, the samples were annealed at 400°C to determine the long-term stability. XRD was used to characterize the phases formed after long-term annealing. Finally, the microstructures of the samples were examined by scanning electron microscopy (SEM, TESCAN MIRA 3 LMH, Czech).

3. Results and discussion

3.1. Physical properties and FT-IR analysis

Fig. 1 shows the effect of the adding content on the physical properties of the oxide-added $\text{A-Na}_2\text{O} \cdot 2\text{SiO}_2$ samples. As shown in Fig. 1 (a), the density of the $\text{A-Na}_2\text{O} \cdot 2\text{SiO}_2$ materials increased with the adding content for the three oxides studied herein. This increase in density after oxides adding can be attributed to the larger molar weight of the adding oxides (Sm_2O_3 , Y_2O_3 , and ZrO_2) as compared to SiO_2 and Na_2O . Besides, at similar adding contents, the density of $\text{A-Na}_2\text{O} \cdot 2\text{SiO}_2$ also increased with the molar weight of the adding oxide. Thus, Sm_2O_3 -added $\text{A-Na}_2\text{O} \cdot 2\text{SiO}_2$ samples showed the largest density among the materials studied herein. To some extent, the density of an amorphous glass is an indicative of the inside network structure and the link degree. Since Y^{3+} , Sm^{3+} , and Zr^{4+} have more electric charges than Na^+ , they can be linked to more non-bridging oxygens. As a result, the number of non-bridging oxygens in the glass network structure decreased, thereby increasing the amount of bridging oxygens and generating a more dense structure after oxide adding.

The effect of oxide-adding on the microhardness of the oxides-added $\text{A-Na}_2\text{O} \cdot 2\text{SiO}_2$ samples is shown in Fig. 1 (b). As in the case of the density, the microhardness increased with the oxide adding content before reaching a maximum value and decreasing thereafter. The Sm_2O_3 - and Y_2O_3 -added $\text{A-Na}_2\text{O} \cdot 2\text{SiO}_2$ materials at 3 mol% showed the highest hardness values. However, in the case of ZrO_2 , the maximum hardness was reached at 2 mol% adding content. Additionally, at similar adding contents, the hardness of the oxides-added $\text{A-Na}_2\text{O} \cdot 2\text{SiO}_2$ materials followed the trend $\text{Y}_2\text{O}_3 > \text{Sm}_2\text{O}_3 > \text{ZrO}_2$. As shown in Fig. 1 (c), similar trends were observed for the elasticity modulus of the oxides-added $\text{A-Na}_2\text{O} \cdot 2\text{SiO}_2$ materials.

The microhardness and elasticity modulus changes can be also explained on the basis of changes in the network structure. Y_2O_3 and

Download English Version:

<https://daneshyari.com/en/article/7217299>

Download Persian Version:

<https://daneshyari.com/article/7217299>

[Daneshyari.com](https://daneshyari.com)